ACS Catalysis

pubs.acs.org/acscatalysis

Research Article

Preparation, Quantification, and Reaction of Pd Hydrides on Pd/Al_2O_3 in Liquid Environment

Thibault Fovanna, Maarten Nachtegaal, Adam H. Clark, Oliver Kröcher, and Davide Ferri*

Cite This: *ACS Catal.* 2023, 13, 3323−3332

Read Online

ACCESS | Metrics & More | Article Recommendations | Supporting Information

ABSTRACT: The ability to study in situ the formation and consumption of Pd hydrides (PdH) in liquid environments is a significant challenge hampering a deeper understanding of catalyzed liquid-phase hydrogenation reactions. Here, using quick scanning X-ray absorption spectroscopy (QEXAFS), we present a detailed kinetic study of Pd hydride formation and reactivity on Pd/Al_2O_3 in 2-propanol solvent. By calibrating the changes in the QEXAFS spectra with temperature-programmed reduction (TPR), we show that the extent of Pd hydride formed or consumed can be assessed quantitatively. This methodology was subsequently used to follow the fate of hydrides during furfural hydrogenation in 2-propanol where their displacement was observed to take place upon coordination of the CO derived from furfural decarbonylation on palladium. The time-resolved quantitative methodology can be used to determine the fraction of Pd hydrides, to assess the kinetics of their displacement and consumption in both the gas and liquid phases.

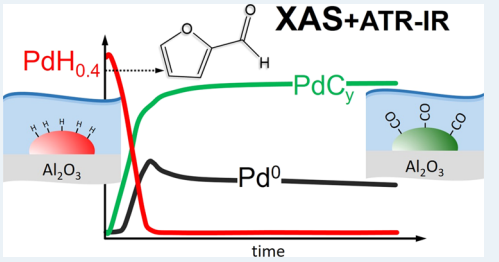

KEYWORDS: *palladium, hydride, carbide, X-ray absorption spectroscopy, temperature-programmed reduction, furfural, 2-propanol, ATR-IR*

INTRODUCTION

Palladium (Pd) is an established active metal for industrial-scale hydrogenation reactions because of its high reactivity and ability to split hydrogen.[1] Pd forms an extensively studied hydride phase due to its hydrogen storage properties.[2,3] Together with the industrial relevance of Pd as a catalyst, the characterization of this hydride phase has been of increasing interest because it has also been identified as the reactive species in hydrogenation reactions[4,5] and electrochemical processes.[4,6] Most relevant characterization studies aiming at the identification and quantification of Pd hydrides (PdH) have been conducted in the gas phase,[4,7,8] while fine chemicals and active pharmaceutical ingredients often rely on liquid-phase catalytic processes.[9] Pd hydrides have been identified in liquid phase under steady-state conditions,[5,10] but their utilization has not been studied so far under in situ or operando conditions in transient experiments. Determination of kinetic rate constants of Pd hydride under defined reactive conditions could help understand solvent properties such as solvent polarity, hydrogen-bonding capability, and steric hindrance affecting the hydride reactivity and stability in the liquid phase.

Three major techniques have been exploited to identify Pd hydrides in the gas phase: transmission electron microscopy (TEM),[11] X-ray diffraction (XRD),[7,12] and X-ray absorption spectroscopy (XAS) at both the K- and L_3-edges.[7,12−14] TEM, XRD, and XAS probe the expansion of the Pd−Pd bonds upon hydride formation. However, in situ TEM studies in liquid environment are challenging because of beam-induced damage. While XRD and XAS do not suffer from major experimental limitations from measurements in liquid phase, they are ambiguous with respect to differentiation between the palladium hydride and carbide phases because lattice expansion is anticipated for both phases in both methods. Hydrides can be identified more easily by characteristic features in X-ray absorption near-edge structure (XANES) spectra at the Pd K-edge.[7] These are typically represented by shifts of the resonances after the absorption edge to lower energy values.[15] The insertion of hydrogen in the Pd−Pd bonds of Pd nanoparticles changes the empty density of states, thus producing characteristic features in the spectra that enable us to distinguish between α-PdH and β-PdH phases in situ.[16] The electronic structure can be addressed more precisely at the Pd L_3-edge,[17] but the presence of the absorbing solvent, absorbing metal oxide support, and cell windows may disfavor in situ measurements. Quantification of hydride stoichiometry has been achieved from extended X-ray absorption fine structure (EXAFS) spectroscopy using an empirical formula

Received: September 28, 2022
Revised: February 3, 2023
Published: February 21, 2023

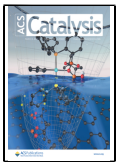

https://doi.org/10.1021/acscatal.2c04791
ACS Catal. 2023, 13, 3323−3332

that is based on the measure of the Pd−Pd bond distance in bulk Pd[8]

$$\Delta R(T)/R_0(T) = 0.0666 \cdot x - 0.0164 \cdot x^2 \quad (1)$$

where $\Delta R(T)$ is the change of the Pd−Pd bond distance induced by hydrogen insertion at a given temperature T, $R_0(T)$ is the Pd−Pd bond distance in the bare (hydrogen free) nanoparticle at T, and x is the H/Pd ratio (PdH_x). Equation 1 is accurate for compositions in the $0 < x < 0.5$ range, but the model relies heavily on the accurate determination of bond distances ($R_0(T)$) from the fit of FT-EXAFS data.[4]

This work is justified because of two reasons. First, as mentioned above the Pd−Pd bond expansion is nonspecific to Pd hydrides and carbides and thus does not allow for unambiguous differentiation between the two phases. Second, Pd K-edge EXAFS is not always experimentally achievable and only the XANES spectrum can be reliably measured. Therefore, an analytical method involving only the XANES region of the XAS spectrum is valuable. Quantification of the hydride phase is key to understand the involvement of hydrides in liquid-phase reaction mechanisms, ideally with sub-second time resolution to determine the kinetics of their formation and consumption. XAS at the Pd K-edge with sub-second time resolution offers the advantage of fast acquisition required to capture such kinetics. Analysis of the large dataset of such time-resolved XAS spectra by multivariate curve resolution alternating least square (MCR-ALS) analysis[18] allows us to extract spectra of the pure components, such as hydride, metallic Pd, PdO, and the carbidic phase as well as to quantify the fractions present at each point in time.

Here, we combine the analysis of time-resolved XAS spectra by MCR-ALS with temperature-programmed reduction (H_2-TPR) as a methodology for in situ quantitative determination of formation and consumption of Pd hydrides in gas- and liquid-phase experiments. This is achieved by combining the time-resolved XAS datasets obtained during hydride formation and desorption in the gas phase and quantification by H_2-TPR. MCR-ALS is then used to extract XAS spectra of the pure components present in all datasets. Finally, the kinetics of hydride consumption during furfural hydrogenation[19] in H_2-saturated 2-propanol was followed by XAS and by attenuated total reflection infrared (ATR-IR) spectroscopy at 50 °C.

EXPERIMENTAL SECTION

Materials and Chemicals. The pre-reduced 5 wt % Pd/Al_2O_3 catalyst used in this study was kindly provided by Chimet (Viciomaggio, Italy) and possessed a surface area of 125 m^2/g. The catalyst was prepared using the method described by Groppo et al.[20] Hydrogen (Carbagas, 99.995% purity), 10 vol % H_2/He (Messer), helium (Carbagas, 99.9999% purity), 5 vol % CO/Ar (Messer), 2-propanol (Merck LiChrosolv hypergrade for LC-MS), and cyclohexene (Sigma-Aldrich, 99%) were used as received. Furfural (Sigma-Aldrich, 99%) was distilled prior to use.

Transmission Electron Microscopy. TEM images were taken using a JEOL 2010 microscope equipped with a LaB_6 filament, an energy-dispersive X-ray spectrometer (EDS, Oxford Instrument), and a charge-coupled device (CCD) camera (Orius from GATAN) with an acceleration voltage of 200 keV. A single tilt holder was used. The sample was prepared by depositing 5 μL of a 2-propanol suspension of the catalyst powder on a holey carbon film supported on a 3 mm copper grid.

Temperature-Programmed Reduction. TPR experiments were carried out in a dedicated instrument (TPDRO 1100, Thermo Scientific) equipped with a thermal conductivity detector (TCD). The sample (600 mg) was loaded at the bottom of a quartz reactor and was kept at 30 °C in a flow of 10 vol % H_2/Ar (20 mL/min) for 15 min prior to heating. TPR profiles were collected in the temperature range of 30−600 °C at a heating rate of 2 °C/min in the same gas flow. The hydrogen consumption and release were quantified from the integration of the peaks area and consideration of a response factor determined using a high-purity CuO standard (Thermo Electron Corporation) under the same conditions.

X-ray Absorption Spectroscopy. Transmission quick scanning X-ray absorption spectra were obtained at the Pd K-edge (24.35 keV) at the SuperXAS beamline of the Swiss Light Source (SLS, Villigen) using 15 cm long ionization chambers filled with 1 bar N_2 and 1 bar Ar. Pd foil, mounted between the second and the third ionization chambers was used for internal energy calibration. The polychromatic beam resulting from the 2.9 T superbent magnet was collimated using a Pt-coated collimating mirror, subsequently monochromatized by a channel-cut Si(111) crystal of the quick scanning monochromator and finally focused using a Pt-coated toroidal mirror to a spot size of 150 μm × 150 μm. Spectra were collected at 1 Hz monochromator oscillation but only the spectra while scanning from low to high energy were considered, resulting in a time resolution of one spectrum per second.

In situ experiments were carried out in a dedicated setup (Figure S1) using a flow cell described previously for gas-phase experiments[21] that was adapted for liquid-phase experiments under pressure and was fitted with two 200 μm thick Teflon windows.[22] This cell was validated for transient experiments in liquid phase (Figures S2−S4). In a typical experiment, the sample (35 ± 1 mg) was firmly fixed between two quartz wool plugs.

During gas-phase experiments, the cell was connected to mass flow controllers delivering a total flow of 20 mL/min. The sample was heated in 10 vol % H_2/He flow from 30 to 170 °C at 2 °C/min and was then kept in these conditions for 15 min prior to switching to He flow and cooling to 30 °C at 2 °C/min.

In liquid-phase experiments, the cell was connected to a high-pressure liquid chromatography (HPLC) pump (10 mL/min stainless steel pump head; Azura P 4.1S; Knauer) delivering solutions at a flow rate of 0.2 mL/min (Figure S1). Two back-pressure regulators (5.2 bar; Upchurch Scientific) were connected in series at the outlet of the cell to achieve a total pressure of 10.4 bar. The sample was made wet at 30 °C with 2-propanol solvent saturated with bubbling H_2 at 1 bar. After pressure equilibration, the cell was heated to 125 °C (10 °C/min) and was then held for 1 h. After reduction, the cell was cooled to 50 °C and the feedstock solution was changed to a H_2-saturated 2-propanol solution of furfural (5 mM), to a H_2-saturated cyclohexane solution of cyclohexene (5 mM), or to CO-saturated 2-propanol. Gas chromatographic analysis of the cell effluent was obtained with a trace gas chromatography (GC) instrument (Thermo Quest) equipped with an HP-5 column (30 m × 0.025 mm × 0.5 μm, Agilent) and a flame ionization detector. Decane was used as an internal standard.

https://doi.org/10.1021/acscatal.2c04791
ACS Catal. 2023, 13, 3323−3332

Quick scanning XAS (quickXAS) spectra were collected throughout the experiments. All spectra were energy-corrected, normalized, and smoothed using ProQEXAFS.[23] Energy calibration was achieved by aligning with the Pd reference foil that was recorded simultaneously with the XAS spectra. The processed time-resolved quickXAS spectra collected during heating in 10 vol % H_2/He, cooling in He, and in the complete liquid-phase experiment were processed all simultaneously with principal component analysis (PCA) by fixing the number of components to three. Then, the whole dataset was fed to the multivariate curve resolution alternating least squares (MCR-ALS) algorithm with the constraints that the components fraction is comprised between 0 and 1 and is non-negative, and that the total concentration of components sums to unity.[24] This approach resides principally in the nature of MCR-ALS, a method that does not require reference spectra and that generates spectra of pure components able to fully describe the system at hand. For this purpose, it requires a dataset with the largest diversity of sample state and composition. Feeding the algorithm with a large number of spectra improves the accuracy of the determination of the representative components of the system. Processing all data together by MCR-ALS ensures also the elimination of biases for example related to ambiguity on whether hydrides deliver the same spectra irrespective of gas and liquid phase. Hence, components are obtained that are able to cope with both reactive environments in a quantitative manner.

Fitting to selected EXAFS spectra was performed using the Demeter software package.[25] Spectra were subjected to background subtraction and converted to the photo-electron wave vector by setting the first inflection point of the absorption edge to 24.35 keV followed by the Fourier transform of the k^2-weighted spectra in the range k = 3−11 Å^{-1}. The first Pd−Pd shell of the EXAFS spectra was fitted using an amplitude reduction factor of 0.83 that was obtained from the fit of a Pd foil reference spectrum.

Linear combination fitting (LCF) analysis of the XANES spectra was performed using the corresponding Prestopronto package using selected spectra as references.[26]

Attenuated Total Reflectance Infrared Spectroscopy. An aqueous suspension of the catalyst (10 mg in 1.5 mL) was stirred for 15 min and deposited on a ZnSe internal reflection element (IRE, 45°, 52 × 20 × 2 mm^3; Crystran) before drying overnight under fume hood. The crystal was loaded in an in-house built ATR-IR cell mounted in the IR spectrometer (Bruker, Vertex 70). The IR spectrometer was equipped with a liquid-nitrogen-cooled mercury cadmium telluride (MCT) detector and a four-mirror ATR assembly (Specac). All spectra were collected at 40 kHz scanner velocity and 4 cm^{-1} resolution by averaging 30 scans. The dry catalyst layer deposited on the ATR crystal was equilibrated at 75 °C for 1 h with a 2-propanol solution saturated with H_2 bubbling at 1 bar prior to cooling to 50 °C until a stable signal was obtained, which was used as background spectrum. Then, a H_2-saturated 2-propanol solution of furfural (5 mM) was allowed to enter the ATR-IR cell while spectra were recorded consecutively. After 30 min, the exiting solution was analyzed by GC as described above. The same procedure was employed for CO adsorption at 50 °C by flowing 2-propanol saturated with 5 vol % CO/Ar bubbling at 1 bar after reduction at 75 °C as described above.

Diffuse Reflectance Infrared Fourier Transform Spectroscopy (DRIFTS). CO adsorption from gas phase was followed by diffuse reflectance infrared Fourier transform spectroscopy (DRIFTS) using a home-made cell[27] fitted with a flat CaF_2 window (d = 25 mm), loaded with the sample and mounted in a Praying Mantis mirror assembly. In analogy to the liquid-phase experiment, the sample was heated in a flow of 5 vol % H_2/Ar to 75 °C and reduced for 1 h prior to cooling to 50 °C and collection of a background spectrum. Then, CO adsorption was monitored for 30 min while flowing 5 vol % CO/Ar and collecting spectra at 10 kHz scanner velocity and 4 cm^{-1} resolution by averaging 100 scans.

RESULTS AND DISCUSSION

The received catalyst sample was composed of Pd nanoparticles of average size 2.5 ± 0.5 nm (Figure S5) dispersed on Al_2O_3 (Figure S6). Despite the reduction treatment performed by the catalyst manufacturer, the reduced state of the Pd nanoparticles was accompanied by ca. 50% of oxidized Pd, most likely due to the prolonged exposure to ambient air, whose presence was discernible in the X-ray absorption near-edge structure spectrum (XANES, Figure S7).

Figure 1 shows the transmission Pd K-edge XANES spectra of 5 wt % Pd/Al_2O_3 collected at 50 °C after reduction in H_2-saturated 2-propanol at 125 °C followed by 30 min exposure to a H_2-saturated solution of furfural (5 mM) together with that of the same catalyst reduced at 125 °C in an identical gas-phase experiment. Comparison with the reference Pd foil suggests that the catalyst was in the reduced state. The visible shift of the oscillations in the spectrum obtained in H_2-saturated 2-propanol to lower energy values can be attributed to the formation of hydrides.[15] This shift can be better appreciated in the difference spectra obtained after subtraction of the spectrum obtained in the gas-phase experiment from the other two spectra (Figure 1). The difference spectra are not featureless as it might be expected upon subtraction of spectra representing the supposedly same state of the Pd component. The oscillations in the difference XANES spectrum related to hydride species are clearly visible in the absence of furfural. These features vanished after introduction of the furfural

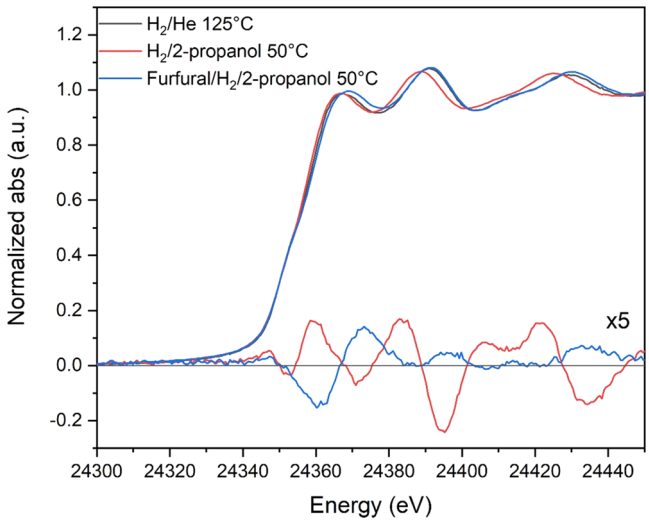

Figure 1. (a) Pd K-edge XANES spectra of 5 wt % Pd/Al_2O_3 in He at 125 °C (black), in H_2-saturated 2-propanol at 50 °C (red), and in H_2-saturated 2-propanol solution of furfural (5 mM) at 50 °C. (b) Difference spectra obtained by subtracting the XANES spectrum obtained in He (black) from the other two spectra.

https://doi.org/10.1021/acscatal.2c04791
ACS Catal. 2023, 13, 3323−3332

Table 1. Fit of the First Pd Shell of the FT-EXAFS Data Obtained in the Liquid-Phase Experiment

	N^a	R (Å)^b	σ^{2c}	ΔE^d	red. χ^{2e}	PdH_x	
IPA[h]/H_2, 125 °C	10.1 ± 0.4	2.794 ± 0.003	0.0100 ± 0.0004	4.2 ± 0.3	47.6	0.36[f]	
IPA/H_2, 50 °C	9.9 ± 0.3	2.804 ± 0.002	0.0086 ± 0.0003	4.2 ± 0.2	36.2	0.43[f]	0.56[g]
FUR[i]/IPA/H_2, 50 °C	9.5 ± 0.4	2.751 ± 0.003	0.0074 ± 0.0004	4.9 ± 0.3	106.5	0.05[f]	0.06[g]

[a]Coordination number. [b]Pd−Pd bond distance. [c]Pseudo Debye−Waller factor. [d]Energy shift. [e]Reduced χ^2. [f]x in PdH_x obtained from eq 1 and EXAFS analysis. [g]x in PdH_x by TPR/MCR-ALS. [h]IPA, 2-propanol. [i]FUR, furfural.

solution, but the corresponding difference spectrum was characterized by a number of other features at different energy than those characteristic of hydrides suggesting the formation of a new phase involving Pd. The apparent opposite shift direction of the spectrum compared to the spectrum of Pd hydrides indicates the possible formation of Pd carbide species or in general the deposition of carbonaceous species that cause the expansion of the Pd lattice to an extent visible by XAS.[7]

Besides XANES, the Fourier transform extended X-ray absorption fine structure (FT-EXAFS) data (Figure S8 and Table 1) also provided evidence of hydride formation from the average value of the Pd−Pd bond distance. Table 1 shows the results for three spectra in similar conditions to those shown in Figure 1. Because the use of EXAFS data in eq 1 requires the knowledge of $R_0(T)$ and $\Delta R(T)$,[8] two gas-phase spectra were obtained at 50 and at 125 °C while cooling in He after reduction at 180 °C. The two spectra should represent bare Pd^0 nanoparticles free of hydrogen. The bond distance of the first Pd neighbor in the spectra is reported in Table 1 together with the corresponding H:Pd stoichiometry determined according to eq 1 and to the methodology described in the following (Figure S9).[8] While the H:Pd stoichiometry obtained by EXAFS fitting and eq 1 is lower than that obtained by a combination of H_2-TPR and XANES, it has to be recalled that eq 1 considers bulk Pd and that Pd nanoparticles may behave differently. Moreover, carbon insertion affects also in a very similar way the average Pd−Pd bond distance determined by EXAFS making this method ambiguous. Hence, XANES appears more reliable and its use is described in the following.

Gas-Phase Experiment. Temperature-programmed reduction by hydrogen (H_2-TPR) was performed to quantify the amount of hydrogen desorbed from and consumed by the catalyst. Figure 2 shows three consecutive TPR measurements from 30 to 180 °C (TPR-1), to 400 °C (TPR-2), and to 600 °C (TPR-3) that served to quantify hydrides in the gas-phase experiment. The aim of the consecutive H_2-TPR was to investigate the effect of the end temperature on the amount of desorbed and consumed hydrogen. Prior to each H_2-TPR experiment, the catalyst was kept in a reducing flow of 10 vol % H_2/Ar for 15 min. The negative peak (H_2 release) centered at 56 °C in the three consecutive H_2-TPR sequences is readily attributed to the desorption of hydrogen from decomposition of hydrides.[20,28] The similar areas of this peak in TPR-1 and TPR-2 suggest that heating the sample to 180 °C did not affect significantly the proportion of the hydride phase. Based on the calibration of the thermal conductivity signal with CuO providing the amount of desorbed hydrogen and on the amount of Pd loaded in the experiment, the H/Pd ratio was 0.4 ($PdH_{0.4}$) for TPR-1 and TPR-2.

In TPR-2 performed up to 400 °C, a positive peak (H_2 consumption) appeared at 260 °C that reflects the reduction of the residual PdO observed by XAS. It corresponds to a H/Pd ratio of 0.07, thus indicating that 7% of Pd remained as PdO

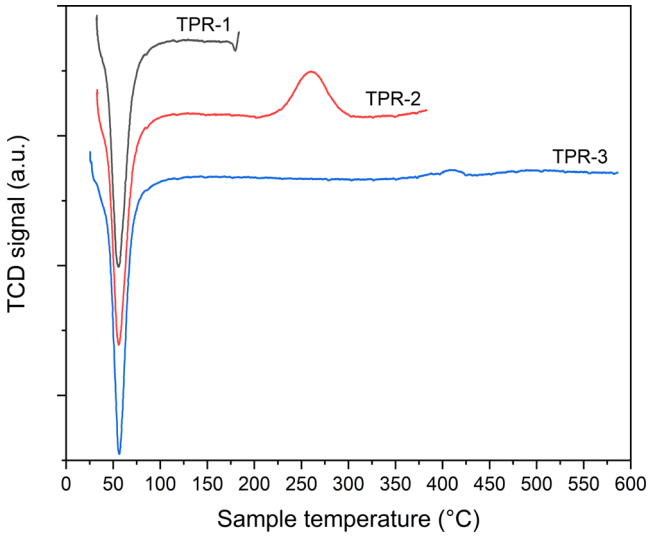

Figure 2. TPR experiments on 5 wt % Pd/Al_2O_3 from 30 to 180 °C (black, TPR-1), 30 to 400 °C (red, TPR-2), and 30 to 600 °C (blue, TPR-3). Conditions: 10 vol % H_2/Ar, 2 °C/min. Profiles are offset for clarity.

and was reduced only at 260 °C. Because more Pd^0 was obtained at the end of TPR-2, the negative peak of hydrides was accordingly larger in TPR-3, while the positive peak at 260 °C was absent indicating unambiguously that Pd reduction was complete after reduction at 400 °C (TPR-2). The amount of desorbed hydride increased from TPR-1/TPR-2 to TPR-3 corresponding to an increase of H/Pd ratio from 0.40 to 0.47, thus consistent with the value of hydrogen consumed for the reduction of PdO in TPR-2. These values of PdH_x are coherent with previous work and are characteristic of the β-PdH phase.[3,4,7,14,29]

Heating and cooling segments of H_2-TPR experiments carried out at different ramping rates (2−5 °C/min; Figure S10) returned values of the energy of desorption and adsorption of H_2 of 1 and 1.3 kJ/mol, respectively, in agreement with the knowledge that hydrogen adsorption−desorption on Pd^0 does not require activation.[30]

The H_2-TPR procedure was repeated in the XAS cell to assign a spectrum to the H:Pd stoichiometry established by the H_2-TPR in Figure 1 on the same sample. Various factors, including particle shape and temperature of reduction, can affect the amount of hydrogen stored in the Pd nanoparticles.[3,28] QuickXAS spectra measured at 30 °C in the 15 min prior to start of the H_2-TPR experiment were analyzed using principal component analysis (PCA) followed by multivariate curve resolution alternating least squares (MCR-ALS; Figure S11). PCA identified three components that allowed describing the reduction of PdO present in the pre-reduced catalyst and the formation of the hydride phase in 10 vol % H_2/He at 30 °C using MCR-ALS. The spectra of the

https://doi.org/10.1021/acscatal.2c04791
ACS Catal. 2023, 13, 3323−3332

three components returned by MCR-ALS (Figure S12a) correspond to Pd^0 (labeled as Pd), Pd hydride, and partially oxidized Pd (PdO). These spectra can be compared to the reference spectra that one would use for a linear combination fit (LCF) of the same dataset (Figure S12b). Because of the nanoparticle nature of Pd, the initial state of the catalyst can be used to represent the partially oxidized state of Pd instead of bulk PdO; in this case, a mixed oxidized state needs to be considered for the initial catalyst (Figure S7). The spectrum of Pd^0 was obtained at 30 °C after H_2-TPR to 400 °C instead of the Pd foil. The spectra of Figure S12 are very similar if not identical, revealing that MCR-ALS delivers the adequate set of components. The spectrum of the fresh sample cannot be considered that of a simple pure component because it is clearly a combination of reduced and oxidized Pd (see above). At 30 °C, the fraction of PdO decreased below 10% within 150 s in the reducing flow (Figure S11) and was replaced by the spectrum of hydrides through a short period (ca. 60 s) of Pd^0 as already observed before.[22]

After reduction at 30 °C, the catalyst was heated to 160 °C to enable observation of desorption of the hydrides by XAS, similar to TPR-1 in Figure 2. Finally, the gas flow was switched to He to obtain the reference spectrum of the bare Pd nanoparticles and the sample was cooled to 30 °C. Pd nanoparticles are termed bare at this point because hydrides have desorbed according to Figure 2. The complete time-resolved XAS dataset measured in the two segments (heating and cooling) was analyzed using MCR-ALS. Figure 3 combines

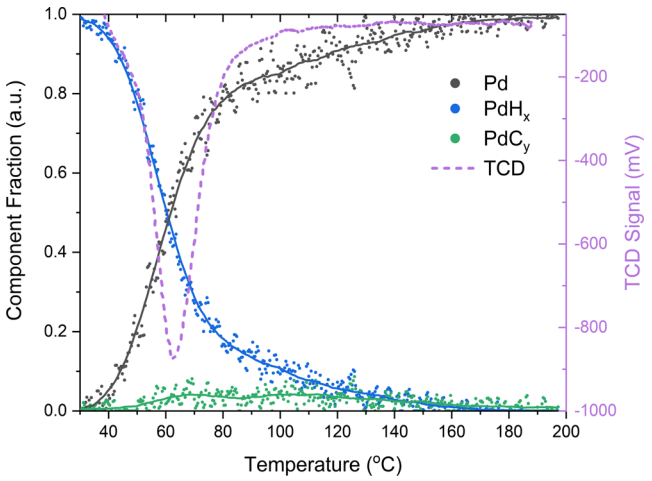

Figure 3. MCR-ALS of in situ XANES spectra of 5 wt % Pd/Al_2O_3 while heating in 10 vol % H_2/He to 160 °C at 2 °C/min. The integrated TCD signal during a similar TPR experiment is also shown.

the integrated area of the TCD signal obtained in TPR-1 and the fraction of hydrides obtained from MCR-ALS analysis of the XAS dataset as a function of temperature during the heating phase. Both curves exhibit essentially the same shape. The difference in desorption temperature (9 °C) obtained from the first derivative of the profiles (Figure S13) is reasonable when considering the differences in geometry and possibly heat distribution between the H_2-TPR reactor and the XAS cell.

The H_2-TPR data in Figure 2 also suggest that hydrides desorbed completely at 110 °C, while the MCR-ALS analysis of the XAS data showed that the hydride component was still present at the same temperature. Similar to TPR-1, heating the sample to 160 °C was not sufficient to remove completely the hydride phase, which may indicate the persistence of the hydride in the α-phase.[13]

Liquid-Phase Experiments. Similar to the gas phase, it was necessary to reduce the oxide phase present on the catalyst in the experiment in the liquid environment. For this purpose, a H_2-saturated 2-propanol solution was passed through the catalyst bed at 125 °C for 1 h. After this reductive treatment, the XANES spectrum of Figure 1 exhibited the same features observed for the Pd hydrides in the gas-phase experiments.[16] However, Figure 3 clearly shows that hydrides begin to desorb below 70 °C in gas-phase experiments. Hence, the stability of hydrides increases significantly in the liquid environment (2-propanol in this case) in the temperature regime where bare Pd^0 is observed in the gas phase, a behavior that we have already observed in the case of Pt/Al_2O_3.[31]

Utilization of the hydrides generated under these experimental conditions is a central topic for liquid-phase-catalyzed hydrogenation reactions.[32] Hence, the above procedure to quantify the fraction of hydrides present on Pd/Al_2O_3 in the liquid environment using MCR-ALS and the dataset of the gas-phase experiments (Figure 3) was repeated by adding the dataset of time-resolved XAS spectra during transient furfural hydrogenation.

The traces in Figure 4a show the temporal evolution of the various Pd species obtained by MCR-ALS starting from the point where a H_2-saturated solution of furfural was admitted to the catalyst bed to enable liquid-phase hydrogenation. Similar to Figure 3 and as described above, the spectra used for MCR-ALS were obtained considering all spectra from the sets of the gas-phase and liquid-phase experiments to improve the robustness of the method (Figure S9). PCA returned up to five principal components but four components were retained (Figure 4b) because they allowed describing a coherent behavior according to the experimental conditions. The spectrum of the fourth component extracted from this dataset presents different features compared to the spectra of PdH_x and PdO species and is attributed to a Pd carbide-like component (PdC_y; Figure 4b). The spectra of pure components were fitted to each spectrum to quantify the fraction of hydrides present. As we can now quantify the H content in the hydride phase, instead of the generic component fraction the right axis scale of Figure 4a shows the actual H:Pd stoichiometry that has been derived from the gas-phase experiment.

At t = 0 min, the initial fraction of hydrides in H_2-saturated 2-propanol at 50 °C was similar to what was achieved in 10 vol % H_2/He at 30 °C in Figure 3 with a hydride fraction of 85% and an initial PdO fraction of 6%, the rest being the Pd^0 component. After switching to the furfural solution, there was a delay of ca. 30 s before changes could be observed in the middle of the catalyst bed, where the spectra were measured, that is associated with the time required for the solution to reach this point. Then, the concentration of hydrides decreased rapidly to zero mirrored by an increasing fraction of the Pd^0 and PdC_y component, which became dominant. Together with the changes associated with Pd^0 and the hydride components, the MCR-ALS analysis returned also the disappearance of the oxidized component (PdO). The features in the XANES spectra after exposure of the catalyst to the furfural solution for 30 min corresponded to those that are considered representative of Pd carbide (or carbonaceous) species as shown in Figure 1, a situation that was achieved already after

https://doi.org/10.1021/acscatal.2c04791
ACS Catal. 2023, 13, 3323−3332

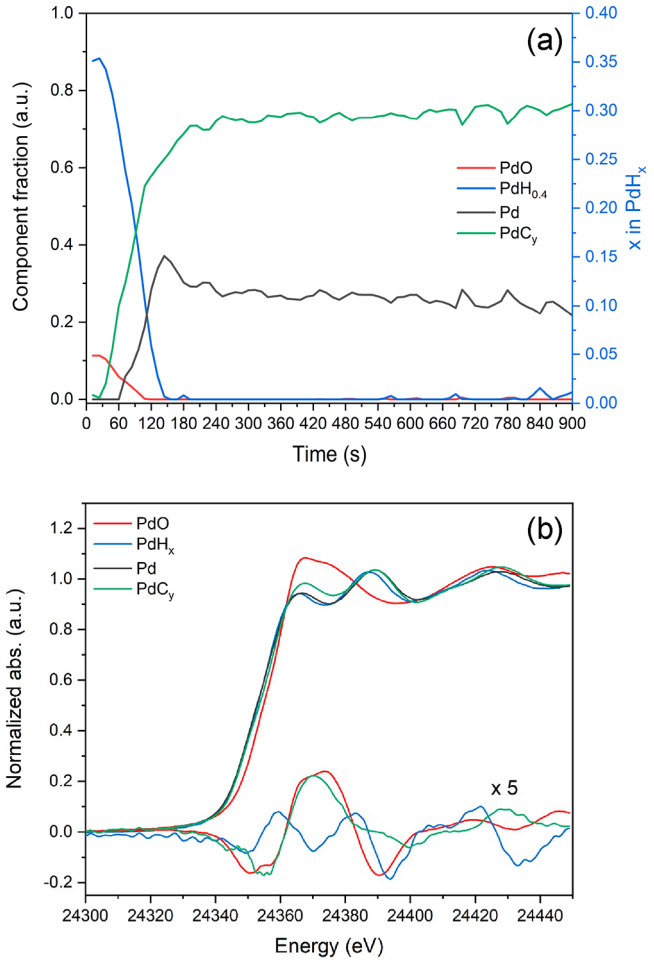

Figure 4. (a) MCR-ALS of in situ XANES spectra of 5 wt % Pd/Al_2O_3 during furfural hydrogenation at 50 °C. PdO (red), Pd (black), and PdH (blue) component fractions are displayed on the left *y*-axis, while H/Pd ratio is displayed on the right *y*-axis. (b) Spectra of pure components used in (a) and scaled difference spectra obtained from subtraction of the spectrum of Pd from the others.

ca. 4 min according to the data of Figure 4.[7] We note that in principle a similar approach to the one shown here could be used for the quantification of these carbidic species in agreement with similar efforts in the gas phase.[7]

To rationalize the behavior of the Pd hydride phase in the presence of furfural, we performed identical measurements at 50 °C with 2-propanol saturated with CO and with a solution of cyclohexene after preparing $PdH_{0.4}$ as described above. The results are shown in Figure 5 from the perspective of the time-dependent XANES data (magnified energy region and 2D time dependence) from the moment the solution containing furfural-H_2, CO, or cyclohexene-H_2 was admitted to the cell. Comparison of the three experiments shows that abrupt changes occurred only in the case of furfural hydrogenation (Figure 5a). Hardly any change was detected in the presence of CO (Figure 5b) and cyclohexene (Figure 5c). The gas chromatographic (GC) analysis of the solution exiting the cell indicated that cyclohexene conversion was 35% after 30 min. Hence, cyclohexene reacted at the surface of the Pd nanoparticles, most likely consuming hydrogen dissociated at their surface. In the case of CO, we anticipate that the ATR-IR spectra obtained in a similar experiment clearly displayed adsorbed CO on reduced Pd (Figure 6), indicating that CO coordinates to the surface of the Pd nanoparticles despite the presence of the hydride phase. In both cases, the XANES data indicated that the supported $PdH_{0.4}$ phase was stable under the applied conditions, while it vanished quickly in the presence of furfural.

We interpret these results using the cartoons in Figure 5. CO adsorption (Figure 5b) is not affected by hydrides, it may displace hydrogen at the surface of the nanoparticles but does not contribute to the removal of the hydrogen atoms present in the particle bulk. Cyclohexene hydrogenation (Figure 5c) most likely uses surface hydrogen atoms and does not affect the bulk of the $PdH_{0.4}$ phase. In this case, an equilibrium is installed that consumes hydrogen atoms through reaction with cyclohexene and that replaces them with new hydrogen atoms from either the bulk hydride phase or directly from the liquid phase. We assume that there is no C-containing deposit here and that cyclohexene adsorbs, reacts, and desorbs as cyclohexane. Therefore, no change is observed in the XANES, which is confirmed by the constant Pd−Pd distance under these conditions observed in the corresponding FT-EXAFS data (not shown). The average size of the Pd particles of this Pd/Al_2O_3 (2.5 nm) is likely already large to allow XAS to become sensitive to surface processes. This is reflected by the high coordination number (CN, ca. 10) obtained by the fit of the FT-EXAFS data in the experiments (Table 1). We interpret the different behavior compared to the experiment with furfural to be given by the desorption of the products of cyclohexene reaction, in this case cyclohexane. In the case of furfural, not only hydrogenation occurred, but likely other side reactions consuming hydrogen atoms took place when furfural was added to the $PdH_{0.4}$ phase that contributed to the consumption of the hydrogen atoms in the particle bulk. The products of these reactions may form a layer of adsorbates that plays the role of barrier preventing hydrogen atoms from maintaining the equilibrium with the bulk, besides reducing the hydrogen coverage. Hydrogen may still dissociate at the Pd surface but cannot enter the bulk, cannot form the $PdH_{0.4}$ phase, and thus cannot be detected by XAS. These adsorbates eventually formed Pd carbide-like species (at least from the perspective of XAS) that are evidently more stable than the starting hydride phase.[33] This interpretation is in line with the electrocatalytic observations of the high reactivity of aldehydes including furfural revealing that bulk hydrides are consumed in the presence of such reactants.[34] However, we believe that in our experiment catalytic activity toward furfural hydrogenation is not sustained by the adsorbates remaining on the catalyst and contributing to PdC_y, rather the catalyst deactivates in a short time. We think that the change in Pd speciation is too abrupt at the point of addition of furfural and that probably the experimental conditions in terms of furfural/Pd ratio are not optimal to achieve stable activity, but this needs to be confirmed with further measurements.

In the case of furfural hydrogenation, GC analysis of the outlet solution revealed that 5% conversion occurred to both furan and furfuryl alcohol, the former being the major product. We have performed a similar operando ATR-IR experiment in a dedicated, hence different, cell that revealed a higher furfural conversion (25%) but similar selectivity under the same conditions of temperature and pressure. The ATR-IR experiment was performed to observe the surface of the Pd/Al_2O_3 catalyst from the perspective of the adsorbates present during furfural hydrogenation. As anticipated above, the spectrum obtained after flowing a furfural solution in H_2-saturated 2-

https://doi.org/10.1021/acscatal.2c04791
ACS Catal. 2023, 13, 3323−3332

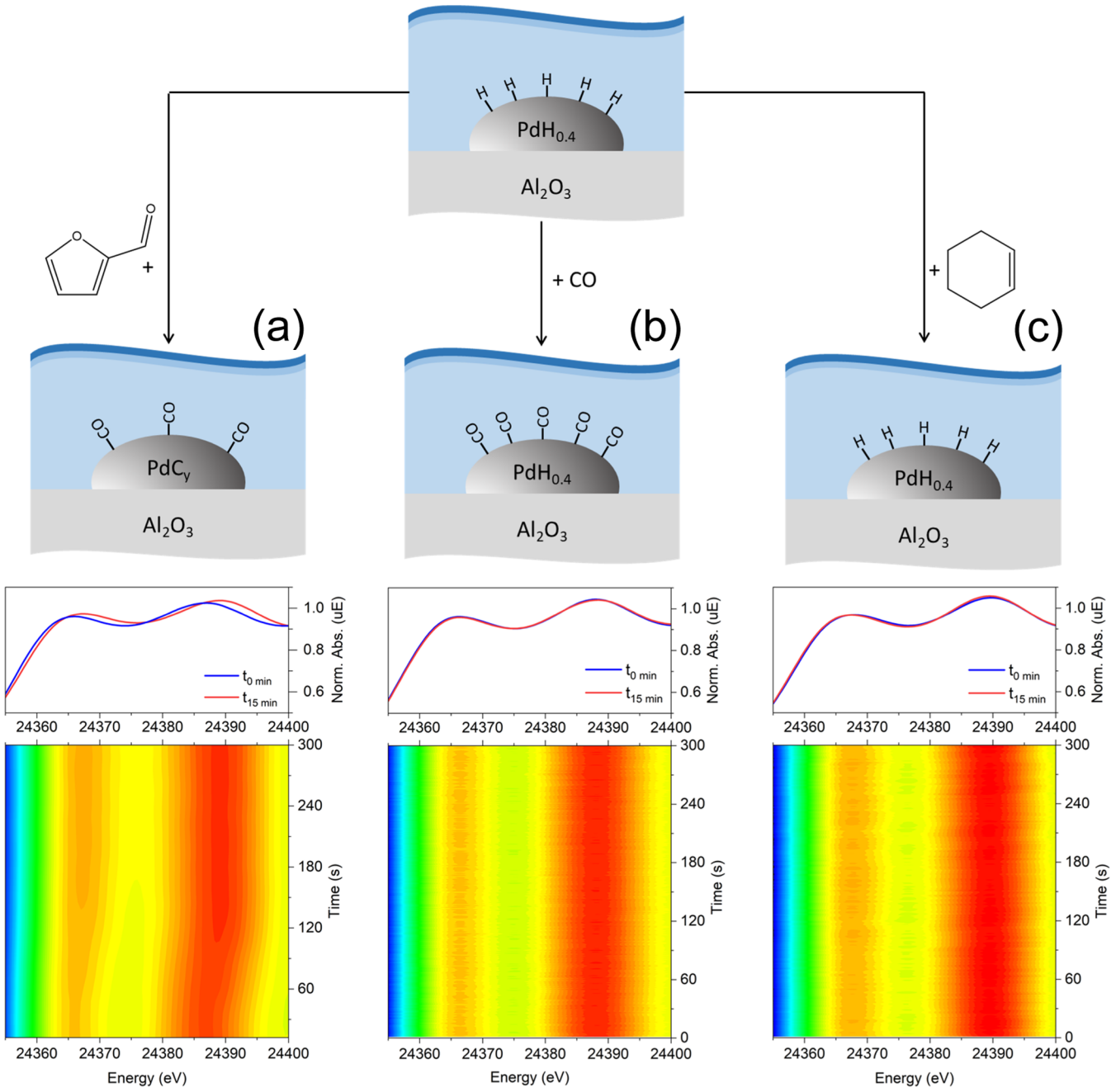

Figure 5. In situ time-resolved XANES spectra of Pd/Al_2O_3 at t = 0 and 15 min and corresponding color map representations of all spectra during (a) furfural hydrogenation (same data of Figure 4), (b) CO adsorption, and (c) cyclohexene hydrogenation after preparation of the supported $PdH_{0.4}$ phase.

propanol for 30 min evidenced the formation of adsorbed CO (Figure 6). The intense band at 1915 cm^{-1} and the weak signal at 2000 cm^{-1} were readily associated with bridged CO (CO_B) and linear bonded CO (CO_L), respectively.[20] The strong CO signals were accompanied by the carbonyl bands (ν(C═O) at 1704 and 1684 cm^{-1})[35] and further signals below 1600 cm^{-1} of dissolved furfural. The first information from the vibrational experiment complementary to the XAS experiment is thus that furfural decarbonylation occurred, in agreement with the identification of furan at the end of both XAS and ATR-IR experiments by GC. The XAS data showed that the hydrides were consumed simultaneously (Figure 5a) and that they were replaced by other species, whose features resemble those of carbide-like species (Figure 1). The ATR-IR spectra do not allow us to assign specific signals to such species suggesting that the carbide-like species are either hidden within the various envelopes (Figure S14) or do not contribute significantly with finite bands. In the latter case, this would point to a nonspecific molecular structure of these species.

Because at this point in time CO covered the Pd surface, CO adsorption from 2-propanol was carried out at 50 °C in the XAS cell after preparing the hydrides as described above. Figure 6 shows also the spectrum obtained at saturation coverage, which displays essentially similar features to those observed in the adsorption of CO during furfural hydrogenation. Figure 5b also demonstrates that CO adsorption did

https://doi.org/10.1021/acscatal.2c04791
ACS Catal. 2023, 13, 3323−3332

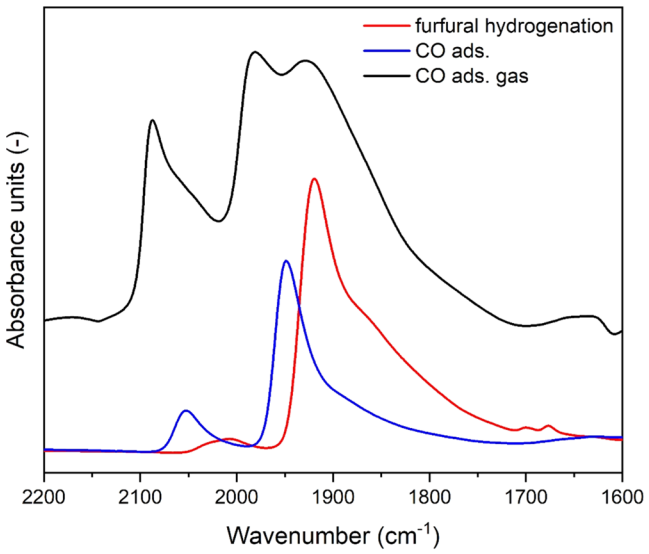

Figure 6. In situ ATR-IR spectra of 5 wt % Pd/Al_2O_3 after 30 min reaction of furfural hydrogenation at 50 °C and after adsorption of CO in 2-propanol at 50 °C (labeled as CO ads.). The DRIFT spectrum of adsorbed CO from gas phase (CO ads. gas) is also shown for comparison and is offset for the sake of clarity.

not displace the hydrides, whose concentration remained constant along the experiment. This is most likely due to the fact that despite the nanosize of the Pd particles, the hydrides are bulk species and poorly interact with CO coordinating to the surface of the particles. Therefore, the removal and consumption of the hydrides must occur because a reaction proceeds at the surface of the particles and its intermediates or byproducts are able to cause the decay of the XAS signal of the hydrides.

Because adsorbed CO observed by ATR-IR spectroscopy during furfural hydrogenation originates from a chemical reaction, it is interesting to compare the CO coverage and the Pd site occupancy with respect to the available Pd surface from both the gas-phase and liquid-phase experiments. The spectrum of adsorbed CO in a gas-phase experiment (5 vol % CO/Ar; Figure 6) was similar to the transmission spectra obtained for the same catalyst.[20] Besides CO_L and CO_B, the hollow bonded CO (CO_H) was present, which appeared as a shoulder of CO_B in 2-propanol, suggesting that CO_H is less favorable in liquid phase. Figure 6 shows that not only adsorption of CO from the gas phase but also adsorption of CO from the liquid phase (CO-saturated 2-propanol) produced a different spectrum from that obtained during furfural hydrogenation. The most striking difference is the bathochromic shift of the CO bands by 20 cm^{-1}. Moreover, the ratio of the integrated areas of the CO_B and CO_L signals (CO_B/CO_L) was 7.7 in the case of CO adsorption in 2-propanol, while it reached a value of ca. 45 in the experiment with furfural suggesting a vastly different site occupancy during reaction.

While we consider that the difference between adsorption of CO from gas phase and from 2-propanol may arise from the different experimental conditions under which adsorption was performed, and also because of the presence of a polar liquid environment (2-propanol), the explanation of the different behavior during reaction and upon CO adsorption in the liquid environment is less straightforward to rationalize. The shift observed during the reaction could be attributed to the presence of hydrogen in the form of hydrides and of furfural, a reactive environment that influences the electronegativity of the surface. This would confirm the observation made by XAS that a fraction of hydrogen remained adsorbed on the Pd surface. We consider the different CO_B/CO_L ratio, an indication that the coverage of Pd(111) sites by CO is lower in the presence of furfural and hydrogen than when only CO is present in solution. This might indicate that the Pd(111) sites that are free of CO can perform furfural hydrogenation to furfuryl alcohol, the competing reaction to the decarbonylation of furfural in the early stages of reaction. At longer reaction times, Rogers et al.[36] showed that catalyst deactivation starts from the carbidization of terrace sites, which could be in agreement with the complete loss of the hydride phase in our experiments in the presence of furfural. The changes in the properties of CO uptake by the Pd nanoparticles observed here are attributed to interaction of adsorbed CO originating from furfural decarbonylation with fragments of organic molecules deriving from furfural (e.g., furans) that contribute probably to the fraction of Pd carbide-like species observed by XANES. The high CO_B/CO_L ratio obtained during reaction is then the result of the removal of the Pd hydride species that is monitored by XAS and that allows a larger coverage of the Pd surface by at least CO, the adsorbate that is clearly visible in the ATR-IR spectra. The co-adsorption of organic moieties probably of aromatic nature could cause increased back-donation to adsorbed CO molecules and elongation of the carbonyl bonds through enhanced electron transfer to the metal nanoparticles,[37] thus potentially justifying the observed bathochromic shift compared to CO adsorption.

CONCLUSIONS

In this work, we have prepared Pd hydrides on a 5 wt % Pd/Al_2O_3 in 2-propanol solvent, we have quantified the H:Pd stoichiometry of the Pd hydrides and we have studied the consumption of Pd hydrides as a result of the chemistry involved in furfural hydrogenation on the catalyst. The determination of the H:Pd stoichiometry was obtained from a similar gas-phase experiment combining H_2 temperature-programmed reduction with X-ray absorption spectra and their multivariate curve resolution alternate least square analysis. This approach does not rely on the use of empiric formulas. During furfural hydrogenation, the Pd hydrides produced on Pd/Al_2O_3 were rapidly consumed and replaced by mixed Pd^0 and Pd carbide-like phases. Rationalization of the results using similar experiments with CO and cyclohexene hydrogenation and complementary data from attenuated total reflection infrared spectroscopy experiments revealed that the bulk hydride phase is readily consumed only in the case of the experiment with furfural. CO and cyclohexene hydrogenation do not contribute to hydride consumption and/or displacement. Therefore, accumulation of furfural hydrogenation and decarbonylation products on the surface of the Pd nanoparticles is associated with the bulk Pd hydride consumption, the carbonaceous byproduct species forming a barrier for bulk hydride formation and preventing achievement of the equilibrium between bulk and surface concentrations of the hydride species. The transient approach proposed in this work to study the reactivity of the Pd hydrides that is borrowed from gas-phase experiments offers new possibilities to interrogate heterogeneous catalytic hydrogenations in the liquid phase.

https://doi.org/10.1021/acscatal.2c04791
ACS Catal. 2023, 13, 3323−3332

■ ASSOCIATED CONTENT

Supporting Information

The Supporting Information is available free of charge at https://pubs.acs.org/doi/10.1021/acscatal.2c04791.

Details of experimental setup and procedure; analysis of residence time distribution of the cell; TEM and particle size distribution; XRD; XANES spectra of pellets of Pd/Al_2O_3, PdO, and Pd foil; radial distribution function of the FT-EXAFS; H_2-TPR experiments at various temperature ramps; MCR-ALS of in situ XANES spectra during gas-phase reduction; spectra of pure components; first derivative of H_2-TPR; and reduction by XAS; ATR-IR spectra during furfural hydrogenation (PDF)

■ AUTHOR INFORMATION

Corresponding Author

Davide Ferri − *Paul Scherrer Institut, CH-5232 Villigen PSI, Switzerland;* orcid.org/0000-0002-9354-5231; Phone: +41 (0)56 310 27 81; Email: davide.ferri@psi.ch

Authors

Thibault Fovanna − *Paul Scherrer Institut, CH-5232 Villigen PSI, Switzerland; Institute of Chemical Sciences and Engineering, École Polytechnique Fédérale de Lausanne (EPFL), CH-1015 Lausanne, Switzerland;* orcid.org/0000-0003-4525-2538

Maarten Nachtegaal − *Paul Scherrer Institut, CH-5232 Villigen PSI, Switzerland;* orcid.org/0000-0003-1895-9626

Adam H. Clark − *Paul Scherrer Institut, CH-5232 Villigen PSI, Switzerland;* orcid.org/0000-0002-5478-9639

Oliver Kröcher − *Paul Scherrer Institut, CH-5232 Villigen PSI, Switzerland; Institute of Chemical Sciences and Engineering, École Polytechnique Fédérale de Lausanne (EPFL), CH-1015 Lausanne, Switzerland;* orcid.org/0000-0002-7268-7257

Complete contact information is available at: https://pubs.acs.org/10.1021/acscatal.2c04791

Notes

The authors declare no competing financial interest.

■ ACKNOWLEDGMENTS

The authors acknowledge the financial support from the Paul Scherrer Institut (CROSS project). The authors are grateful to G. Garin for support with experiments, Dr. R. Pellegrini (Chimet S.p.A.) for providing the sample and for useful discussions, Dr. I. Alxneit for the TEM measurements, and the SLS for beamtime allocation at the SuperXAS beamline.

■ REFERENCES

(1) Chen, B.; Dingerdissen, U.; Krauter, J. G. E.; Lansink Rotgerink, H.; Möbus, K.; Ostgard, D. J.; Panster, P.; Riermeier, T. H.; Seebald, S.; Tacke, T.; Trauthwein, H. New Developments in Hydrogenation Catalysis Particularly in Synthesis of Fine and Intermediate Chemicals. *Appl. Catal., A* **2005**, *280*, 17−46. Augustine, R. L. *Heterogeneous Catalysis for the Synthetic Chemist*; CRC Press, 1995.

(2) Graham, T. On the Absorption and Dialytic Separation of Gases by Colloid Septa. *Philos. Trans. R. Soc. London* **1866**, *156*, 399. Dekura, S.; Kobayashi, H.; Kusada, K.; Kitagawa, H. Hydrogen in Palladium and Storage Properties of Related Nanomaterials: Size, Shape, Alloying, and Metal-Organic Framework Coating Effects. *ChemPhysChem* **2019**, *20*, 1158−1176. Flanagan, T. B.; Oates, W. A. The Palladium-Hydrogen System. *Annu. Rev. Mater. Sci.* **1991**, *21*, 269−304. Jewell, L. L.; Davis, B. H. Review of absorption and adsorption in the hydrogen−palladium system. *Appl. Catal., A* **2006**, *310*, 1−15. Sakintuna, B.; Lamari-Darkrim, F.; Hirscher, M. Metal Hydride Materials for Solid Hydrogen Storage: A Review. *Int. J. Hydrogen Energy* **2007**, *32*, 1121−1140.

(3) Kishore, S.; Nelson, J. A.; Adair, J. H.; Eklund, P. C. Hydrogen Storage in Spherical and Platelet Palladium Nanoparticles. *J. Alloys Compd.* **2005**, *389*, 234−242.

(4) Siebel, A.; Gorlin, Y.; Durst, J.; Proux, O.; Hasché, F.; Tromp, M.; Gasteiger, H. A. Identification of Catalyst Structure during the Hydrogen Oxidation Reaction in an Operating PEM Fuel Cell. *ACS Catal.* **2016**, *6*, 7326−7334.

(5) Chase, Z. A.; Fulton, J. L.; Camaioni, D. M.; Mei, D.; Balasubramanian, M.; Pham, V. T.; Zhao, C.; Weber, R. S.; Wang, Y.; Lercher, J. A. State of Supported Pd during Catalysis in Water. *J. Phys. Chem. C* **2013**, *117*, 17603−17612.

(6) Diercks, J. S.; Herranz, J.; Georgi, M.; Diklic, N.; Chauhan, P.; Ebner, K.; Clark, A. H.; Nachtegaal, M.; Eychmüller, A.; Schmidt, T. J. Interplay between Surface-Adsorbed CO and Bulk Pd Hydride under CO_2-Electroreduction Conditions. *ACS Catal.* **2022**, *12*, 10727−10741.

(7) Bugaev, A. L.; Guda, A. A.; Lazzarini, A.; Lomachenko, K. A.; Groppo, E.; Pellegrini, R.; Piovano, A.; Emerich, H.; Soldatov, A. V.; Bugaev, L. A.; et al. In Situ Formation of Hydrides and Carbides in Palladium Catalyst: When XANES Is Better than EXAFS and XRD. *Catal. Today* **2017**, *283*, 119−126.

(8) Feenstra, R.; Griessen, R.; deGroot, D. G. Hydrogen Induced Lattice Expansion and Effective H-H Interaction in Single Phase PdHc. *J. Phys. F: Met. Phys.* **1986**, *16*, 1933.

(9) Joshi, S. S.; Ranade, V. V. *Industrial Catalytic Processes for Fine and Specialty Chemicals*; Elsevier, 2016; p 756.

(10) Selinsek, M.; Deschner, B. J.; Doronkin, D. E.; Sheppard, T. L.; Grunwaldt, J. D.; Dittmeyer, R. Revealing the Structure and Mechanism of Palladium during Direct Synthesis of Hydrogen Peroxide in Continuous Flow Using Operando Spectroscopy. *ACS Catal.* **2018**, *8*, 2546−2557.

(11) Wang, J.; Wang, Q.; Jiang, X.; Liu, Z.; Yang, W.; Frenkel, A. I. Determination of Nanoparticle Size by Measuring the Metal−Metal Bond Length: The Case of Palladium Hydride. *J. Phys. Chem. C* **2015**, *119*, 854−861.

(12) Bugaev, A. L.; Guda, A. A.; Lomachenko, K. A.; Lazzarini, A.; Srabionyan, V. V.; Vitillo, J. G.; Piovano, A.; Groppo, E.; Bugaev, L. A.; Soldatov, A. V.; et al. Hydride Phase Formation in Carbon Supported Palladium Hydride Nanoparticles by in Situ EXAFS and XRD. *J. Phys.: Conf. Ser.* **2016**, *712*, No. 012032.

(13) Dekura, S.; Kobayashi, H.; Ikeda, R.; Maesato, M.; Yoshino, H.; Ohba, M.; Ishimoto, T.; Kawaguchi, S.; Kubota, Y.; Yoshioka, S.; et al. The Electronic State of Hydrogen in the α Phase of the Hydrogen-Storage Material PdH(D)x: Does a Chemical Bond Between Palladium and Hydrogen Exist? *Angew. Chem., Int. Ed.* **2018**, *57*, 9823−9827.

(14) Bugaev, A. L.; Srabionyan, V. V.; Soldatov, A. V.; Bugaev, L. A.; vanBokhoven, J. A. The Role of Hydrogen in Formation of Pd XANES in Pd-Nanoparticles. *J. Phys.: Conf. Ser.* **2013**, *430*, No. 012028.

(15) McCaulley, J. A. In-situ X-ray Absorption Spectroscopy Studies of Hydride and Carbide Formation in Supported Palladium Catalysts. *J. Phys. Chem. A* **1993**, *97*, 10372−10379.

(16) Bugaev, A. L.; Guda, A. A.; Lomachenko, K. A.; Srabionyan, V. V.; Bugaev, L. A.; Soldatov, A. V.; Lamberti, C.; Dmitriev, V. P.; vanBokhoven, J. A. Temperature- and Pressure-Dependent Hydrogen Concentration in Supported PdHx Nanoparticles by Pd K-Edge X-Ray Absorption Spectroscopy. *J. Phys. Chem. C* **2014**, *118*, 10416−10423.

(17) Tew, M. W.; Miller, J. T.; vanBokhoven, J. A. Particle Size Effect of Hydride Formation and Surface Hydrogen Adsorption of Nanosized Palladium Catalysts: L3 Edge vs K Edge X-ray Absorption Spectroscopy. *J. Phys. Chem. C* **2009**, *113*, 15140−15147.

(18) Cassinelli, W. H.; Martins, L.; Passos, A. R.; Pulcinelli, S. H.; Santilli, C. V.; Rochet, A.; Briois, V. Multivariate Curve Resolution Analysis Applied to Time-Resolved Synchrotron X-Ray Absorption Spectroscopy Monitoring of the Activation of Copper Alumina Catalyst. *Catal. Today* **2014**, *229*, 114−122.
(19) Mariscal, R.; Maireles-Torres, P.; Ojeda, M.; Sadaba, I.; Granados, M. L. Furfural: A Renewable and Versatile Platform Molecule for the Synthesis of Chemicals and Fuels. *Energy Environ. Sci.* **2016**, *9*, 1144−1189.
(20) Groppo, E.; Agostini, G.; Piovano, A.; Muddada, N. B.; Leofanti, G.; Pellegrini, R.; Portale, G.; Longo, A.; Lamberti, C. Effect of Reduction in Liquid Phase on the Properties and the Catalytic Activity of Pd/Al_2O_3 Catalysts. *J. Catal.* **2012**, *287*, 44−54.
(21) Chiarello, G. L.; Nachtegaal, M.; Marchionni, V.; Quaroni, L.; Ferri, D. Adding Diffuse Reflectance Infrared Fourier Transform Spectroscopy Capability to Extended X-Ray-Absorption Fine Structure in a New Cell to Study Solid Catalysts in Combination with a Modulation Approach. *Rev. Sci. Instrum.* **2014**, *85*, No. 074102. Marchionni, V.; Kambolis, A.; Nachtegaal, M.; Kröcher, O.; Ferri, D. High energy X-ray diffraction and IR spectroscopy of Pt/Al_2O_3 during CO oxidation in a novel catalytic reactor cell. *Catal. Struct. React.* **2017**, *3*, 71−78.
(22) Fovanna, T.; Alxneit, I.; Clark, A. H.; Checchia, S.; Michiel, M. D.; Kröcher, O.; Nachtegaal, M.; Ferri, D. Reduction of PdO/Al_2O_3 in liquid cyclohexane followed in situ by ATR-IR, high energy XRD and XAS. *J. Phys. Chem. C* **2021**, *125*, 16473−16482.
(23) Clark, A. H.; Imbao, J.; Frahm, R.; Nachtegaal, M. ProQEXAFS: A Highly Optimized Parallelized Rapid Processing Software for QEXAFS Data. *J. Synchrotron Radiat.* **2020**, *27*, 551−557.
(24) Jaumot, J.; deJuan, A.; Tauler, R. MCR-ALS GUI 2.0: New Features and Applications. *Chemom. Intell. Lab. Syst.* **2015**, *140*, 1−12.
(25) Ravel, B.; Newville, M. ATHENA, ARTEMIS, HEPHAESTUS: Data Analysis for X-Ray Absorption Spectroscopy Using IFEFFIT. *J. Synchrotron Radiat.* **2005**, *12*, 537−541.
(26) http://soonready.github.io/PrestoPronto/ (accessed Nov 17, 2022).
(27) Nuguid, R. J. G.; Kröcher, O.; Ferri, D. Design of a reactor cell for modulated excitation Raman and diffuse-reflectance studies of selective catalytic reduction Catalysts. *Emiss. Control Sci. Technol.* **2019**, *5*, 307−316.
(28) Sá, J.; Arteaga, G. D.; Daley, R. A.; Bernardi, J.; Anderson, J. A. Factors Influencing Hydride Formation in a Pd/TiO_2 Catalyst. *J. Phys. Chem. B* **2006**, *110*, 17090−17095.
(29) Paleček, D.; Tek, G.; Lan, J.; Iannuzzi, M.; Hamm, P. Characterization of the Platinum−Hydrogen Bond by Surface-Sensitive Time-Resolved Infrared Spectroscopy. *J. Phys. Chem. Lett.* **2018**, *9*, 1254−1259.
(30) Niemantsverdriet, J. W. *Spectroscopy in Catalysis: An Introduction*; Wiley-VCH Verlag GmbH & Co. KGaA, 2007; p 344.
(31) Carosso, M.; Fovanna, T.; Ricchebuono, A.; Vottero, E.; Manzoli, M.; Morandi, S.; Pellegrini, R.; Piovano, A.; Ferri, D.; Groppo, E. Gas phase vs. liquid phase: monitoring H_2 and CO adsorption phenomena on Pt/Al_2O_3 by IR spectroscopy. *Catal. Sci. Technol.* **2022**, *12*, 1359−1367.
(32) Aireddy, D. R.; Ding, K. Heterolytic Dissociation of H2 in Heterogeneous Catalysis. *ACS Catal.* **2022**, *12*, 4707−4723.
(33) García-Mota, M.; Bridier, B.; Perez-Ramirez, J.; Lopez, N. Interplay between carbon monoxide, hydrides, and carbides in selective alkyne hydrogenation on palladium. *J. Catal.* **2010**, *273*, 92−102.
(34) Meyer, L. C.; Sanyal, U.; Stoerzinger, K. A.; Koh, K.; Fulton, J. L.; Camaioni, D. M.; Gutierrez, O. Y.; Lercher, J. A. Influence of the Molecular Structure on the Electrocatalytic Hydrogenation of Carbonyl Groups and H_2 Evolution on Pd. *ACS Catal.* **2022**, *12*, 11910−11917. Singh, N.; Sanyal, U.; Ruehl, G.; Stoerzinger, K. A.; Gutierrez, O. Y.; Camaioni, D. M.; Fulton, J. L.; Lercher, J. A.; Campbell, C. T. Aqueous Phase Catalytic and Electrocatalytic Hydrogenation of Phenol and Benzaldehyde over Platinum Group Metals. *J. Catal.* **2020**, *382*, 372−384.
(35) Allen, G.; Bernstein, H. J. Internal Rotation VIII. The Infrared and Raman Spectra of Furfural. *Can. J. Chem.* **1955**, *33*, 1055−1061.
(36) Rogers, S. M.; Catlow, C. R. A.; Chan-Thaw, C. E.; Chutia, A.; Jian, N.; Palmer, R. E.; Perdjon, M.; Thetford, A.; Dimitratos, N.; Villa, A.; Wells, P. P. Tandem Site- and Size-Controlled Pd Nanoparticles for the Directed Hydrogenation of Furfural. *ACS Catal.* **2017**, *7*, 2266−2274.
(37) Bonalumi, N.; Vargas, A.; Ferri, D.; Baiker, A. Theoretical and Spectroscopic Study of the Effect of Ring Substitution on the Adsorption of Anisole on Platinum. *J. Phys. Chem. B* **2006**, *110*, 9956−9965. Cruz, M. T. d. M.; Carneiro, J. W. d. M.; Aranda, D. A. G.; Bühl, M. Density Functional Theory Study of Benzene Adsorption on Small Pd and Pt Clusters. *J. Phys. Chem. C* **2007**, *111*, 11068−11076. Morin, C.; Simon, D.; Sautet, P. Chemisorption of Benzene on Pt(111), Pd(111), and Rh(111) Metal Surfaces: A Structural and Vibrational Comparison from First Principles. *J. Phys. Chem. B* **2004**, *108*, 5653−5665.

https://doi.org/10.1021/acscatal.2c04791
ACS Catal. 2023, 13, 3323−3332